

**Pressure and Temperature Dependence of Reaction Kinetics and Product
Branching in the Reaction of Vinyl Radical (C₂H₃) with Ethylene**

Pui-Teng Howe,^a Paul R. Abel,^b Huzeifa Ismail,^c Claude F. Goldsmith,^b Askar Fahr,^{*,d}
Joshua Halpern,^d Leonard E. Jusinski,^e Yuri Georgievski,^e Craig A. Taatjes,^{*,e}
William H. Green Jr.^{*,b}

^a *Department of Chemistry, American University, Washington, DC 20016;* ^b *Department of Chemical Engineering, Massachusetts Institute of Technology, Cambridge, MA 02139;*
^c *Department of Chemistry, Massachusetts Institute of Technology, Cambridge, MA 02139;* ^d *Department of Chemistry, Howard University, Washington D.C., 20059;*
^e *Combustion Research Facility, Mail Stop 9055, Sandia National Laboratories, Livermore, CA 94551-0969*

Abstract This work reports direct kinetics and product studies of the C₂H₃ + C₂H₄ reaction. Direct kinetic studies were performed over a temperature range of 300 K to 700 K and pressures of 20 mbar and 133 mbar. Vinyl radicals (H₂C=CH) were generated by laser photolysis of vinyl iodide (C₂H₃I) at 266 nm and time-resolved absorption spectroscopy was used to probe vinyl radicals through the absorption at 423.2 nm. The experimental rate constant at 133 mbar was determined to be: $k = 10^{-10.05 \pm 0.07} \exp(-(2384 \pm 83) \text{ K}/T) \text{ cm}^3 \text{ molecules}^{-1} \text{ s}^{-1}$. Product studies were performed at 523 K, 623 K and 723 K, over a pressure range of 27 mbar to 933 mbar. Gas chromatographic and mass spectrometric analysis, with flame ionization detection, was used for product studies. Formation of 1-butene, 1,3-butadiene, 1,5-hexadiene, cyclohexene, acetylene, 1,7-octadiene, and an unidentified product of molecular mass 82 was observed. The product yields show a complex pressure and temperature dependence. The yields of 1,3-butadiene and cyclohexene increase with temperature while the yields of 1-butene and 1,5-hexadiene decrease as temperature is increased. Kinetic modeling of the reaction system,

* Authors to whom correspondence should be addressed. Electronic mail afahr@msrce.howard.edu (Askar Fahr), cataatj@sandia.gov (Craig A. Taatjes), whgreen@mit.edu (William H. Green, Jr.)

based on automated reaction mechanism generation and on literature calculations of stationary points on the C₄H₇ potential energy surface (Miller, J. L., *J. Phys. Chem. A* **2004**, 108, 2268) has been performed to rationalize the observed pressure and temperature dependence of the product yields.

Introduction

The reactions of hydrocarbons at high temperature are central to understanding of the combustion chemistry as well as petroleum processing. Vinyl radical ($\text{H}_2\text{C}=\text{CH}\cdot$) reactions play an important role in hydrocarbon pyrolysis and combustion processes.¹ Ethylene is the simplest olefin, hence its thermal chemistry serves as the basis for understanding the thermal chemistry of other olefins. At temperatures below 1000 K, C_2H_4 decomposition proceeds primarily through disproportionation to give C_2H_5 and C_2H_3 .^{2,3} Although the chemistry of C_2H_5 is fairly well understood, the chemistry of C_2H_3 remains relatively unknown. For example, there have been few direct studies of the kinetics and product branching of the important C_2H_3 self-reaction, four at 298 K^{4, 5, 11,12,13} and one at 623 K,¹⁴ although a number of studies have treated the combination / disproportionation channels of the vinyl self-reaction based on modeling complex reaction systems.⁵⁻¹⁰

An understanding of the $\text{C}_2\text{H}_3 + \text{C}_2\text{H}_4$ reaction system will help elucidate a more accurate description of the C_2H_4 pyrolysis in particular and olefin pyrolysis in general. In addition, polyethylene is one of the most important synthetic polymers. It is a widely used multi purpose material and has the largest annual production among all synthetic commodity polymers. In recent years, gas phase polymerization has emerged as the most versatile process for the production of polyethylene. However, the fundamental microscopic processes involved in gas phase ethylene polymerization are not well understood.¹⁵ The reaction between the vinyl radical and ethylene,



has potential importance as the initiating and/or propagating step in gas phase ethylene polymerization. Surprisingly, there have been only very limited studies on the $\text{C}_2\text{H}_3 + \text{C}_2\text{H}_4$ reaction to date.

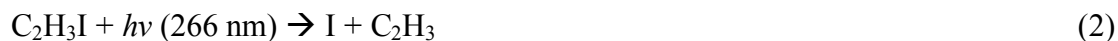
Fahr and Stein¹⁶ employed the Very Low Pressure Pyrolysis (VLPP) technique to study the kinetics and products of the $C_2H_3 + C_2H_4$ reaction over a temperature range of 1023-1273 K and at low pressure between 1.3 - 13 μ bar. The temperature dependent rate parameters for the $C_2H_3 + C_2H_4$ reaction were derived relative to the vinyl self- reaction, $C_2H_3 + C_2H_3$. More recently, Shestov and coworkers¹⁷ reported the kinetic studies of the $C_2H_3 + C_2H_4$ reaction from 625-950 K and at pressures between 7 and 15 mbar, using the Laser Photolysis/Photoionization Mass Spectroscopy (LP/PIMS) technique. Under the conditions of these two previous studies only C_4H_6 and C_4H_7 were detected as the major products. Both of the previous studies were done under conditions of low pressures and high temperature. The goal of the present study was to confirm the earlier results, measure pressure dependence, extend to lower temperature and analyze products as a function of pressure and temperature.

In the present work, the kinetics and product channels of the reaction of C_2H_3 with C_2H_4 have been studied over a temperature range of 300 K to 723 K, and for pressures ranging from 27 mbar to 933 mbar. The product studies employed excimer laser photolysis to generate the vinyl radicals and GC/MS/FID product analysis methods, for identifying and quantifying the final products. The yield of products were determined at various temperature and total pressure conditions as well as with various ethylene partial pressure. The reaction system is modeled using known and estimated rate parameters and the simulated product yields at various conditions are compared with the experimental values.

Experimental Procedures

A: Kinetic Studies

The kinetics experiments on the title reaction were performed in the Massachusetts Institute of Technology's Combustion Dynamics Laboratory. Vinyl radical (C_2H_3) is generated via flash photolysis of vinyl iodide at 266 nm:



Photolysis pulses are generated by frequency-doubling the 532 nm output of a short pulse Nd:YAG. The optical arrangement is represented in Figure 1.

Direct absorption by vinyl radical is used to monitor the reaction of vinyl + ethylene. Vinyl radicals are detected by multiple pass laser absorption at 423.3 nm.¹⁸ The detection wavelength is generated using a mode-locked Ti:Sapphire laser (1.2 ps at 80 MHz) pumped by a 532 nm diode-pumped solid state continuous-wave (CW) laser. The output of the Ti:Sapphire laser is frequency-doubled using a BBO crystal or frequency-converted using an OPO crystal producing an overall spectral range of 230 – 1200 nm.

The picosecond Ti:Sapphire Laser be easily tuned through its entire spectral range, without any major changes to the optical path. A high resolution spectrometer (0.1 nm FWHM) is used to determine the output wavelength. The probe laser is treated as quasi-CW, with FWHM resolution of $\sim 13 \text{ cm}^{-1}$. This resolution limits studies to molecules with broad absorption features. The vinyl radical is an ideal system for such an apparatus, because it offers absorption feature observable to our probe laser, yet narrow enough to allow tuning off resonance, as shown in Figure 2.

The experiment is carried out in a 160 cm long temperature-controlled stainless steel flow reactor. An internally mounted Herriott-type multiple pass cell provides an overall probe path length of up to 40 m allowing detection of transient absorptions of ~ 0.0001 , corresponding to [absorption cross section \times concentration] less than $1 \times 10^{-7} \text{ cm}^{-1}$. To improve the signal-to-noise ratio, a balanced detection scheme is used where the reference beam (I_0) is normalized to and subtracted from the probe beam (I) using a continuously variable optical attenuator and a low noise differential amplifier.

Calibrated mass flow controllers are used to maintain a constant flow of the reactant and buffer gases. The internal pressure of the reactor is measured by a capacitance manometer and controlled with an automated butterfly valve. Both the flow

controllers and automatic butterfly valve are set and adjusted via computer interface. The flow reactor is heated in a ceramic oven. Heat tape is used to supply additional heat to the reactor entrance and exit region. The entrance, center, and exit temperatures are monitored using K-type thermocouples which are fed into three independent PID controllers to maintain a constant temperature. The apparatus is shown in Figure 1.

The kinetics experiments were performed between 300 K and 700 K at high pressure (133.3 mbar) and between 500 K and 700 K at low pressure (20 mbar). To maintain pseudo-first-order conditions, ethylene concentrations (5×10^{16} to 8×10^{17} molecules cm^{-3}) were in large excess to vinyl ($\sim 2 \times 10^{12}$ molecules cm^{-3}). For most of the experiments, vinyl iodide concentrations were maintained at $[\text{C}_2\text{H}_3\text{I}] = 1 \times 10^{15}$ molecules cm^{-3} . Some experiments were performed at several concentrations of vinyl by varying photolysis laser intensity and $\text{C}_2\text{H}_3\text{I}$ concentration. It was found that the rate constants did not depend on $[\text{C}_2\text{H}_3]$, confirming the validity of a pseudo-first-order approximation.

To determine k_1 , the decay rate of C_2H_3 was measured as a function $[\text{C}_2\text{H}_4]$. Values of k_1 were obtained in the usual manner as the slope of a plot of the pseudo-first order rate constant for vinyl loss, k' (where $k' = k_1 [\text{C}_2\text{H}_4] + k_2$), versus $[\text{C}_2\text{H}_4]$. The effective rate constant k_2 is attributable to all other loss processes for vinyl radical, including reaction with the photolytic precursor, diffusion out of the beam, and heterogeneous loss. Plotting k' vs. $[\text{C}_2\text{H}_4]$ yielded lines of constant slope as shown in Figure 3. The uncertainty limits of k' shown in Fig. 3 represent the statistical uncertainty resulting from the fit of the C_2H_3 decay data to a single exponential.

B: Product Studies

The experimental methods used to study product formation in the vinyl + ethene reaction have been described elsewhere,¹⁹ hence only a brief description will be given here.

Vinyl radicals were generated from excimer laser photolysis at 248 nm of vinyl iodide ($\text{C}_2\text{H}_3\text{I}$). Dilute mixtures of $\text{C}_2\text{H}_3\text{I}$ ($7 \times 10^{13} \text{ cm}^{-3}$ to $3 \times 10^{15} \text{ cm}^{-3}$) and C_2H_4 ($7 \times 10^{15} \text{ cm}^{-3}$ to $3 \times 10^{17} \text{ cm}^{-3}$) in He (27 mbar to 933 mbar) were irradiated in a cylindrical temperature-controlled quartz reaction cell (10 cm long, with 2 cm inner diameter). The reaction cell was heated using clam-shell heaters. Sample temperatures of up to 723 K can be achieved with a temperature gradient of less than 4 % across the cell. To minimize the photolysis of the products, the photolyzed reaction mixture was removed by circulation of the reaction mixture in an enclosed loop using a self-enclosed pump. The active photolysis volume was about 0.3 % of the total volume of the loop. Photolysis times were typically 15 min at a repetition rate of 1 Hz or 30 min at a repetition rate of 0.5 Hz. The laser energy was typically 200 mJ per pulse as measured at the source. Under these conditions, the C_2H_3 radical concentrations generated from photolysis typically range from 6×10^{11} to $3 \times 10^{13} \text{ molecules cm}^{-3}$. These radical concentrations were determined from gas chromatographic measurements of the $\text{C}_2\text{H}_3\text{I}$ loss due to photolysis.

In experiments where the total pressure was varied, the $\text{C}_2\text{H}_3\text{I} / \text{C}_2\text{H}_4 / \text{He}$ ratio was kept constant at 0.2:20:700 while only the total pressure was changed. The C_2H_4 partial pressure in these experiments was 27 mbar. In the experiments where C_2H_4 partial pressure was changed, the $\text{C}_2\text{H}_3\text{I}$ concentration and the total pressure were kept constant. The product analysis studies were carried out at temperatures of 523 K, 623 K and 723 K, for pressures ranging from 27 to 933 mbar.

Reaction products were separated, identified and quantified using an on-line gas chromatography/mass spectroscopy (GC/MS) system, interfaced with a flame ionization detector (FID) and a quadrupole mass spectrometer. Calibration of retention times, response factors and comparison of cracking patterns using known standard samples enabled positive identification of the products. However, absolute quantification proved elusive because of uncharacterized, possibly species-dependent, loss of products from secondary reactions; the carbon balance of products was well below 50%. As a result,

whereas the product identification gives a reliable measure of the temperature and pressure dependence of each observed product, absolute experimental branching fractions are not reported.

The vinyl iodide sample was commercially purchased at the highest purity commercially available (up to 95%). The main impurity in the vinyl iodide sample was tetrahydrofuran, which has negligible absorption at 248 nm. Removal of tetrahydrofuran from the sample by distillation is not feasible because the boiling points of tetrahydrofuran and vinyl iodide are very similar. Analysis of the reaction products showed no indication of tetrahydrofuran involvement. The vinyl iodide samples were used after successive freeze-pump-thaw cycles and without further purification. Ethylene (99.999 %) was used without further purification.

Even at the highest temperature of this product study (723 K), ethylene does not undergo significant pyrolysis. However, ethylene undergoes slight photolysis (1% to 2%) at temperatures above 623 K. The primary products of ethylene photochemistry at 248 nm are 1-butene and 1,3-butadiene. As these are also products of the $\text{C}_2\text{H}_3 + \text{C}_2\text{H}_4$ reaction, in order to account for the contributions from ethylene photochemistry, control experiments were performed where ethylene was irradiated in the reaction cell in the absence of vinyl iodide. In this way, the contributions from ethylene photochemistry can be accounted for. Similarly no significant thermal decomposition of vinyl iodide was observed at lower temperatures of this study. However, at 723 K, there was $\approx 1\%$ thermal decomposition over the duration of the typical photolysis time (15-30 min). The extent of thermal decomposition was insignificant compared to the extent of the laser photolysis. The contributions to the products from the $\text{C}_2\text{H}_3\text{I}$ pyrolysis and photolysis were assessed through a number of controlled experiments vinyl iodide/He samples were irradiated in the absence of ethylene or kept in the heated reaction cell without irradiation.

C: Modeling Method

The kinetics studies for the primary reaction were modeled using a RRKM master equation approach, using the VariFlex program package [VariFlex]. The optimized geometries and zero-point corrected energies for the C_4H_7 isomers and the transition states calculated by Miller [Miller] were used as the starting point. The simplified potential energy surface for the vinyl + ethylene reaction was similar to that employed by Shestov et al. [Shestov], and includes the 3-buten-1-yl, 1-methylallyl, and 1-buten-1-yl isomers of the C_4H_7 radical as well as the vinyl + ethylene and $H + 1,3$ -butadiene bimolecular channels. The frequencies and rotational constants for the entrance barrier transition state and the transition state between 1-methylallyl and $H + 1,3$ -butadiene were calculated using CASPT2(5e,5o)/aVDZ method. Additional quantum calculations for hindered rotations were calculated (using Gaussian 03 [Gaussian]) at the B3LYP/6-311G(d,p) level. Each hindered rotor was treated as a 1-d classical hindered rotor, with barriers to hindered internal rotation fit to Fourier series. Tunneling through an Eckart barrier was included for all transition states. Shestov et al. found that raising the energy for the entrance transition state from Miller's value by $1.3 \text{ kcal mol}^{-1}$ gave good agreement with experiment. In the present case, a much smaller increase, $0.4 \text{ kcal mol}^{-1}$, would provide a good fit to the experimental rate constants. This correction is within the accuracy of the G3 method used by Miller. The present master equations predict a smaller branching to the 1-methylallyl radical than suggested by Shestov et al., with less than about 10 % of the reaction forming the resonance-stabilized species.

The reaction mechanism for the product analysis was generated using RMG, an open-source automatic reaction model generating program [RMG refs]. The algorithm for mechanism generation is described in detail in [RMG]. Thermodynamic parameters and high-pressure-limit rate parameters are stored in a hierarchical database based on functional groups. Thermodynamic parameters for specific molecules are included in a primary thermodynamic library, and thermodynamic properties for all other molecules

are estimated using group additivity. RMG's kinetics database is divided into 34 reaction families. Small molecule oxidation reactions that cannot be described by reaction families are included in a primary reaction library. The temperature, pressure, and initial concentrations of vinyl radical, ethylene, and helium were provided to RMG as input; it was assumed that 1% of the initial vinyl iodide is photolyzed to form the vinyl radical. RMG calculates the high-pressure limit for all the rate constants in the mechanism. The rate constants pertaining to the vinyl + ethylene PES were added as a reaction library, which automatically overwrites the RMG-generated high-pressure rate constant with the pressure-dependent rate constants generated from the master equation calculations.

Results and Discussion

A: Kinetic Measurements

The Arrhenius plot of k_1 is shown in Figure 4. An Arrhenius fit to the measured rate coefficient for reaction 1 at 133 mbar yields

$$k_1 = 10^{-10.05 \pm .07} \times \exp(-(2384 \pm 83) \text{ K} / T) \text{ cm}^3 \text{ molecules}^{-1} \text{ s}^{-1} \quad (3)$$

and a fit to the present results at 20 mbar gives

$$k_1 = 10^{-10.21 \pm .21} \times \exp(-(2336 \pm 340) \text{ K} / T) \text{ cm}^3 \text{ molecules}^{-1} \text{ s}^{-1} \quad (4)$$

The error limits in the Arrhenius expressions are the uncertainty determined from the linear fit of the k' data only.

The reaction of vinyl radical with ethylene has been investigated by several authors. The results from all these studies have been summarized in Table 1. The previous experiments were generally carried out at conditions of lower pressure and higher temperature than the present experiments. Benson and Haugen [??] and Fahr and Stein [??] indirectly determined the rate constant for reaction (1) via kinetic modeling of the ethylene pyrolysis study performed by Skinner and Sokoloski [??]. This T-dependent

rate is approximately a factor 10 lower the results from many of the recent studies including the current work [xx, xx].

The activation energy from an Arrhenius fit to the data taken at 133 mbar is found to be $4.74 \text{ kcal mol}^{-1}$ and that at 20 mbar is found to be $4.64 \text{ kcal mol}^{-1}$. The difference between these values is well within experimental uncertainty. These activation energies are approximately 1 kcal mol^{-1} lower than the activation energy obtained from an Arrhenius fit to the data of Shestov et.al.¹⁷ and $\sim 1 \text{ kcal mol}^{-1}$ greater than the entrance barrier calculated by Miller²⁰.

As seen in Figure 4, the present data at 20 mbar agrees with Shestov's data, whereas the rate coefficient at 133 mbar appears consistently $\sim 20\% - 30\%$ higher at all temperatures, suggesting the vinyl + ethylene reaction is in the falloff region at the present experimental conditions and those of Shestov et al.. The results of the master equation calculations are also shown in Figure 4; a very slight falloff is predicted by the master equation simulations, with $k_1(6.65 \text{ mbar}) \sim 15\%$ smaller than $k_1(133 \text{ mbar})$ at 700 K.

One of the intriguing aspects of the vinyl + ethene reaction in the context of molecular weight growth and soot formation in combustion is the possibility of forming resonance-stabilized C_4H_7 radicals. Resonance-stabilized radicals are less reactive than their unstabilized isomeric counterparts, and tend to reach larger concentrations in flames. As a result, resonance-stabilized radicals, in particular the propargyl (C_3H_3) radical, play a prominent role in aromatic formation and soot production. Miller²⁰ predicted formation of delocalized 1-methylallyl isomer in the vinyl + ethylene reaction. Shestov et al. concluded from the thermal stability of the observed C_4H_7 product that substantial 1-methylallyl formation occurs in the reaction, and carried out master equation simulations that suggested 40 % of the reaction proceeded by this pathway under the conditions of their experiments. The present master equation calculations predict somewhat smaller 1-methylallyl yields that (in general) rise with temperature and

fall with increasing pressure, as shown in Figure X. An attempt was made to directly observe 1-methylallyl radical in the laser absorption experiments. Koshi²¹ found allyl radical absorption to be in the same region as vinyl (370-420 nm). It is to be expected that 1-methylallyl would also have absorption bands in this region, except that it may be more diffuse. Under the conditions of high temperature (650 K), low pressure (20 mbar), and high ethylene concentration, a low resolution spectrum of this system was taken from 390 nm to 440 nm. However, no features appeared that could be attributed to absorption by a 1-methylallyl reaction product. The visible absorption cross sections of vinyl radical and allyl radical are similar, and the signal-to-noise for the vinyl radical under these conditions is > 20 . However, the master equation simulations predict a relatively small yield of 1-methylallyl under these conditions, and it is possible that a 1-methylallyl yield consistent with the calculations simply is too small to be observed. Higher sensitivity measurements, possibly in other wavelength regions, may be required to observe absorption from 1-methylallyl produced in this reaction.

B: Product Studies

The addition reaction between vinyl radical and ethylene is expected to initially lead to the 3-buten-1-yl ($\text{CH}_2\text{CHCH}_2\text{CH}_2$) radical adduct. The reaction can also lead to the less stable 1-buten-1-yl radical ($\text{CHCHCH}_2\text{CH}_3$), or to the more stable 3-methylallyl radical $\text{CH}_2\text{CHCHCH}_3$, either via chemical activation or by isomerization of the initially formed $\text{CH}_2\text{CHCH}_2\text{CH}_2$ radical. The excited C_4H_7^* can also decompose to $\text{C}_4\text{H}_7^* \rightarrow \text{C}_4\text{H}_6$ (1,3-butadiene) + H.

For the $\text{C}_2\text{H}_3 + \text{C}_2\text{H}_4$ reaction under very low pressures and high temperature conditions of earlier studies^{16,17} the only products identified were C_4H_7 and C_4H_6 . Under the conditions of the present measurements, the primary products will suffer subsequent reaction before the stable final products are detected. Acetylene, 1,3-butadiene 1-butene, 1,5-hexadiene, cyclohexene and 1,7-octadiene have been identified in this product study.

In addition, an unidentified product of molecular weight of 82 was also detected. Product yields were normalized relative to the initial concentration of C_2H_3 radical, determined from the loss of C_2H_3I . It is likely that the major products, 1-butene, 1,3-butadiene, 1,5-hexadiene and cyclohexene are formed mainly from the reactions of C_4H_7 radicals. For the lowest pressures used in these studies, regardless of temperature, 1,3-butadiene appears to be the dominant product. This is reasonable since the reaction $C_4H_7^* \rightarrow C_4H_6 + H$ is likely to be a major channel for butadiene formation, which should be more efficient at low pressures. Under high pressure conditions however, due to stabilization of $C_4H_7^*$, bimolecular reactions of C_4H_7 become more significant increasing the 1,5-hexadiene yield, while the 1,3-butadiene yield would become less significant.

The rule-based estimates in the RMG model predict the secondary chemistry based on families of known reactions, and the RMG mechanism therefore provides a framework for interpreting the pressure and temperature dependence of the observed stable products in terms of the primary products of the vinyl + ethylene reaction.

The primary stable product 1,3-butadiene is observed directly. The yield of 1,3-butadiene generally decreases with increasing pressure and increases with increasing temperature, consistent with production via a bimolecular channel in competition with stabilization. The measured yield increases slightly with increasing ethylene partial pressure, and levels off for $[C_2H_4]$ above approximately 15 mbar. Figure 5 shows the experimental and RMG-modeled yield of 1,3-butadiene versus total pressure. The full set of measured yields is available as supplementary material. The decrease of the 1,3-butadiene yields with increasing pressure is poorly captured by the RMG model; the computed branching to 1,3-butadiene + H in the vinyl + ethene reaction is rather low under the conditions of the product yield experiments, and much of the 1,3-butadiene in the RMG mechanism arises from secondary or side chemistry, including $H + C_4H_7$.

The yield of 1-butene versus total pressure at selected temperatures is plotted in Figure 7. The contributions from the ethylene photochemistry to the 1-butene yield has

been deducted from the total 1-butene yield. As illustrated in Figure 7, at 523 K, 1-butene yield rises rapidly with pressure, reaching a maximum at around 200 mbar. Above 200 mbar pressure however the 1-butene yield decreases. At 623 K, 1-butene yield shows a broad maximum centered around 500 mbar. Interestingly, at high temperatures the 1-butene yield reaches a negligible level. The RMG mechanism predicts too high a concentration of 1-butene, perhaps for similar reasons as for the overestimate of 1,3-butadiene; both 1-butene and 1,3-butadiene may be products of H atom reactions with C_4H_7 and it is possible that the H-atom chemistry is inaccurately modeled in the automatically generated mechanism.

The stabilized C_4H_7 radicals predicted to be the major products of the reaction of vinyl with ethylene will yield various C_6H_{10} isomers from reactions with ethylene and isomers of C_8H_{14} from recombination reactions. Figure 9 displays the observed and RMG-modeled yield of 1,5-hexadiene versus total pressure. The 1,5-hexadiene is a likely product of the 3-buten-1-yl radical with ethylene. At 523 and 623 K, 1,5-hexadiene yield increases with pressure up to about 300-400 mbar and then decreases at higher pressures. The yield of 1,5-hexadiene decreases as temperature is increased. At 723 K, 1,5-hexadiene yield increases with pressure up to about 300 mbar and remains nearly unchanged at higher pressures. The RMG model captures the qualitative behavior of the 1,5-hexadiene yields and reasonably matches the quantitative yields, although the increased removal of 1,5-hexadiene at higher pressures is poorly modeled. One conceivable reason for the decrease in experimental yield at high pressure could be that 1,5-hexadiene isomerizes to form other C_6H_{10} isomers. If 1,5-hexadiene were to increasingly isomerize to form cyclohexene and/or the unidentified C_6H_{10} isomer as pressure is increased from 533 to 933 mbar, the experimental yields of the latter would increase as 1,5-hexadiene yield decreases. However, the yields of all three C_6H_{10} isomers, 1,5-hexadiene, cyclohexene and the unidentified isomer decrease from 533 to 933 mbar.

Cyclohexene is a conceivable product of addition of either major C_4H_7 isomer to ethylene followed by ring formation and H-atom elimination. The yield of cyclohexene versus total pressure at a number of temperatures is plotted in Figure 11. At 523 K, cyclohexene yield increases with pressure to a broad maximum centered around 100-200 mbar. As pressure is further increased, the yield appears to decrease. Cyclohexene yield increases rapidly with increasing temperature from 523 K to 623 K. The yields at 623 K and 723 K, are comparable at pressures up to about 300 mbar. The yield at 623 K decreases rapidly from its maximum at about 300 mbar while that at 723 K reaches a later maximum at about 500 mbar and decreases thereafter. The yield of cyclohexene also continues to rise with increasing ethylene concentration at least to partial pressures of 55 mbar, suggesting that secondary reactions with ethylene may play a role in its formation. The RMG model predicts very small concentrations of cyclohexene???????? Cyclohexene product can also be formed by isomerization of 1,5-hexadiene (or other hexadienes).

Other isomers of C_6H_{10} may be expected to arise from 1-methylallyl reactions with ethene, for example 1,4-hexadiene or 3-methyl-1,4-pentadiene. However, these isomers are not directly observed in the experiments, although one product of molecular mass 82 remains unidentified. The yield of the unidentified mass-82 product versus total pressure is shown in Figure 13. At 523 K and 623 K, the yield increases with pressure up to about 300 mbar and then decreases at higher pressure. The rate of the initial rise decreases with increasing temperature. At 723 K, the yield reaches a maximum around 300 mbar, above which it remains nearly constant. As with cyclohexene, the yield of the unidentified product increases monotonically with ethylene partial pressure. This unidentified product has a molecular weight of 82 and is likely to be another isomeric form of 1,5-hexadiene such as 3-methyl 1,4-pentadiene, 1,3- or 2,4- hexadiene. The RMG model predicts concentrations of 1,3-hexadiene at nearly the levels of 1,5-hexadiene, and 2,4-hexadiene somewhat lower, but still substantial. 3-methyl-1,4-pentadiene can also be

formed from the reaction of vinyl with the $\text{CH}_2\text{CHCHCH}_3$ isomeric form of C_4H_7 . Standard samples of these other potential product molecules were not available for reference and calibration. Although at least three isomers of C_6H_{10} are observed, positive identification of products of 1-methylallyl remains elusive.

In addition to the above major reaction products, a small quantity of 1,7-octadiene was also observed which most likely is produced through $\text{C}_4\text{H}_7 + \text{C}_4\text{H}_7 \rightarrow \text{C}_8\text{H}_{14}$ reaction. Figure 15 shows the yield of 1,7-octadiene at 523 K and $P = 27$ mbar, 200 mbar and 933 mbar. The yield increases monotonically with pressure. This yield is modeled fairly well by the RMG mechanism. However, the RMG mechanism also predicts similar or larger concentrations of other C_8H_{14} isomers, such as 2,6-octadiene, that may be expected to result from recombination reactions of the 1-methylallyl radical, or reactions of 1-methylallyl with 3-buten-1-yl. These isomers remain unobserved experimentally; again no clear experimental evidence is observed for 1-methylallyl formation.

Conclusions:

The reaction kinetics and product channels of the $\text{C}_2\text{H}_3 + \text{C}_2\text{H}_4$ reaction have been studied at temperatures ranging from 300 K to 723 K and over a pressure range of 27 to 933 mbar. An Arrhenius fit to the present measurements for this reaction at 133 mbar yields

$$k_1 = 10^{-(10.05 \pm .07)} \times \exp(- (2384 \pm 83) \text{ K} / T) \text{ cm}^3 \text{ molecules}^{-1} \text{ s}^{-1} \quad (3)$$

and at 20 mbar yields

$$k_1 = 10^{-(10.21 \pm .21)} \times \exp(- (2336 \pm 340) \text{ K} / T) \text{ cm}^3 \text{ molecules}^{-1} \text{ s}^{-1} \quad (4)$$

The current results at 20 mbar qualitatively agree with results of Fahr and Stein¹⁶ and Shestov et al.¹⁷ The rate constant measured at 133 mbar is consistently higher than both the rate constant at 20 mbar and the data of Shestov et al., suggesting the vinyl + ethylene

reaction is in the falloff region in the present work and at the lower pressure conditions of Fahr and Stein and Shestov et al.'s studies.

The major final reaction products detected in this work are acetylene, 1-butene, 1,3-butadiene, 1,5-hexadiene, cyclohexene and 1,7-octadiene, as well as an unidentified C_6H_{10} isomer. The product yields show complex and significant pressure and temperature dependences. The products can be rationalized by a kinetic model employing RRKM/master equation simulations based ab initio calculations of relevant stationary points; however, experimental evidence for resonance-stabilized radical formation remains ambiguous at best.

Acknowledgments:

This work is supported by the Division of Chemical Sciences, Geosciences, and Biosciences, the Office of Basic Energy Sciences (BES), the U. S. Department of Energy (DOE). Part of the work of A.F. and P-T. H. was supported by DOE/BES contract #DE-FG02-02ER15360. Sandia is a multi-program laboratory operated by Sandia Corporation, a Lockheed Martin Company, for the National Nuclear Security Administration under contract DE-AC04-94-AL85000.

Figure Captions

Figure 1. Diagram of experimental apparatus.

Figure 2. The red trace is on resonance of C_2H_3 at 423.2 nm. The blue trace is off resonance taken at 418.0 nm. The inset shows a vinyl spectrum reprinted with permission from Shahu et. al.⁴

Figure 3. Pseudo-first-order C_2H_3 decay rate k' vs. $[C_2H_4]$, at a temperature of 550 K and a total density of 3.05×10^{18} molecules cm^{-1} . The inset (a) shows the recorded decay of C_2H_3 for the conditions $[C_2H_4] = 1 \times 10^{18}$ molecules cm^{-1} (circles) and $[C_2H_4] = 2.2 \times 10^{18}$ molecules cm^{-1} (squares). Every 100th point is shown for clarity.

Figure 4. Temperature dependence of the rate of the title reaction. Triangles: experimental results of the current study under high pressure conditions; circles: experimental results of the current study under low pressure conditions; squares: results reported by Shestov et. al. in [17]. Dash-dot lines are the Arrhenius fits for each data set.

Figure 5. Yield of 1-butene versus total pressure.

Figure 6. Yield of 1-butene versus ethylene partial pressure.

Figure 7. Yield of 1,3-butadiene versus total pressure.

Figure 8. Yield of 1,3-butadiene versus ethylene partial pressure.

Figure 9. Yield of 1,5-hexadiene versus total pressure.

Figure 10. Yield of 1,5-hexadiene versus ethylene partial pressure.

Figure 11. Yield of cyclohexene versus total pressure.

Figure 12. Yield of cyclohexene versus ethylene partial pressure.

Figure 13. Yield of unidentified product (M.W.=82) versus total pressure.

Figure 14. Yield of unidentified product (M.W.=82) versus ethylene partial pressure.

Figure 15. Yield of 1,7-octadiene versus total pressure.

Figure 16. Simulated yield of 1-butene versus total pressure.

Figure 17. Simulated yield of 1,3-butadiene versus total pressure.

Figure 18. Simulated yield of 1,5-hexadiene versus total pressure.

Figure 19. Simulated yield of 1,7-octadiene versus total pressure.

Table 1: Comparison of Vinyl + Ethylene rate constant of previous studies and current study

	Method	Temperature range (K)	Pressure (mbar)	A-factor (cm ³ molecule ⁻¹ s ⁻¹)	E_a/R (K)
Benson and Haugen ²² (1967)	Thermochemical Estimate	1170-1430		8.3×10^{-13}	0
Fahr and Stein ¹⁶ (1989)	VLPP	1023-1273		1.04×10^{-12}	1560
Miller ²⁰ (2004)	Computational Quantum Chemistry				1810 ^a
Shestov ¹⁷ (2005)	LP/PIMS	625-950	7 - 15	2.04×10^{-12}	2830 ± 790
Current Study	Laser photolysis / Laser absorption	300-700	133	8.9×10^{-11}	2384 ± 83
		500-700	20	6.2×10^{-11}	2336 ± 340

^a Relative enthalpy of transition state on potential energy surface.

References

1. Tsang W. and Hampson R. F., *J. Phys. Chem. Ref. Data* **1986**, *15*, 1087.
2. Sakai T. *In Pyrolysis: theory and industrial practice. Edited by* L. F. Albright, B. L. Crynes, and W. H. Corcoran. Academic Press, New York, 1983. pp. 89-116.
3. Roscoe J. M., Bossard A. R. and Back M. H. *Can J. Chem.* **2000**, *78*, 16.
4. Thorn R. P., Payne W. A., Stief L. J. and Tardy D. C., *J. Phys. Chem.* **1996**, *100*, 13594 and references therein.
5. Fahr A., Braun W. and Laufer A. H., *J. Phys. Chem.* **1993**, *97*, 1502.
6. Tickner A. W. and Le Roy D. J., *J. Chem. Phys.* **1951**, *19*, 1247.
7. Sherwood A. G. and Gunning H. E. *J. Phys. Chem.* **1965**, *69*, 2323.
8. Weir N. A. *J. Chem. Soc.* **1965**, 6870.
9. Takita S., Mori Y. and Tanaka I. *J. Phys. Chem.* **1968**, *72*, 4360.
10. Szirovicza L. *Int. J. Chem. Kinet.* **1985**, *17*, 117.
11. Fahr A., Laufer A. H., Klien R. and Braun W. J. *J. Phys. Chem.* **1991**, *95*, 3218.
12. Fahr A. and Laufer A. H. *J. Phys. Chem.* **1990**, *94*, 726.
13. MacFadden K. O. and Currie C. L. *J. Chem. Phys.* **1973**, *58*, 1213.
14. Kubitz C. Ph.D. Thesis, Technische Hochschule Darmstadt, Darmstadt, Germany, 1995.
15. Xie T., McAuley K. B., Hsu J. C. C. and Bacon D. W., *Ind. Eng. Chem. Res.*, **1994**, *33*, 449.
16. Fahr A., Stein S. E., *Proc. Combust. Inst.*, **1989**, *22*, 1023.
17. Shestov A. A., Popov K. V., Slagle I. R., Knyazev V. D., *Chem. Phys. Lett.*, **2005**, 408, 339.

18. Shahu M., Yang C. H., Pibel C. D., McIlroy A., Taatjes C. A., Halpern J. B., *J. Chem. Phys. Lett.*, **2002**, 116, 8343.
19. Howe P. T. and Fahr A., *J. Phys. Chem. A* **2003**, 107, 9603.
20. Miller, J.L., *J. Phys. Chem. A* **2004**, 108, 2268.
21. Tonokura, K., Koshi, M., *J. Phys. Chem. A* **2000**, 37, 8456.
22. Benson S. W. and Haugen G. R., *J. Phys. Chem.* **1967**, 71, 1735.
23. Howe P. T. and Fahr A. unpublished results. (20)
24. Tsang W. and Hampson R. F. *J. Phys. Chem. Ref. Data* **1986**, 15, 1087. (21)
25. Kiefer J. H., Mitchell K. I. and Wei H. C. *Int. J. Chem. Kinet.* **1988**, 20, 787. (22)
26. Weissman M. and Benson S. W. *Int. J. Chem. Kinet.* **1984**, 16, 307. (23)
27. (a) Bayrakceken F., Brophy J. H., Fink R. D. and Nicholas J. E. *J. Chem. Soc. Faraday Trans. 1* **1973**, 69, 228. (24).
(b) Mitchell T. J. and Benson S. W. *Int. J. Chem. Kinet.* **1993**, 25, 931.
28. Roth W. R., Bauer F., Beitat A., Ebbrecht T. and Wustefeld M. *Chem. Ber.* **1991**, 124, 1453. 25
29. Dean A. M. *J. Phys. Chem.* **1985**, 89, 4600. 26
30. Fahr A. *Int. J. Chem. Kinet.* **1995**, 27, 769. 27
31. Tsang W. *J. Phys. Chem. Ref. Data* **1991**, 20, 221. 28
32. Baulch D. L., Cobos C. J., Cox R. A., Esser C., Frank P., Just Th., Kerr J. A., Pilling M. J., Troe J., Walker R. W. and Warnatz J. *J. Phys. Chem. Ref. Data* **1992**, 21, 411. 29